HHS Public Access

Author manuscript

Toxicol Appl Pharmacol. Author manuscript; available in PMC 2023 December 15.

Published in final edited form as:

Toxicol Appl Pharmacol. 2022 December 15; 457: 116314. doi:10.1016/j.taap.2022.116314.

Oxidative stress modulates expression of immune checkpoint genes via activation of AhR signaling

Ziyue Kou[1], **Rui Yang**[1], **Eunji Lee**[1], **Suresh Cuddapah**[1], **Byeong Hyeok Choi**[1,**], **Wei Dai**[1,**]

[1]Department of Environmental Medicine, Grossman School of Medicine, New York University, 341 East 25th Street, New York, NY 10010

Abstract

Reactive oxygen species (ROS) are by-products of metabolism of oxygen and they play an important role in normal homeostasis and cell signaling, as well as in the initiation of diseases including cancer when their production is upregulated. Thus, it is imperative to understand the cellular and molecular basis by which ROS impact on various biological and pathological processes. In this report, we show that human keratinocyte cell line (HaCaT) treated with hydrogen peroxide displayed an increased activity of AhR, leading to enhanced expression of its downstream targets including cytochrome P450 genes. Intriguingly, preincubation of the complete culture medium with hydrogen peroxide accelerated AhR activation and its downstream signaling. Subsequent mass spectrometric analysis reveals that the oxidant elicits the production of oxindole, a tryptophan catabolic product. We further demonstrate that 2-oxindole (a major form of oxindole) is capable of activating AhR, strongly suggesting that ROS may exert a significant impact on AhR signaling. Consistent with this, we also observe that hexavalent chromium [Cr(VI)], a heavy metal known to generate ROS *in vivo*, enhances AhR protein levels, as well as stimulates expression of CYP1A2 in an AhR-dependent manner. Significantly, we show that hydrogen peroxide and 2-oxindole induce expression of IDO1 and PD-L1, two immune checkpoint proteins. Given the role of IDO1 and PD-L1 in mediating T cell activity and/or differentiation, we postulate that ROS in the tumor microenvironment may play a crucial role in immune suppression via perturbing AhR signaling.

**Co-correspondences: Dr. Wei Dai and Byeong Hyeok Choi, Wei.dai@nyulangone.org, ByeongHyeok.choi@nyulangone.org.

Declaration of interests

The authors declare that they have no known competing financial interests or personal relationships that could have appeared to influence the work reported in this paper.

CRediT author statement

Ziyue Kou: Investigation, Formal analysis, Writing - Original Draft, **Rui Yang**: Investigation Eunji Lee: Validation **Suresh Cuddapah:** Supervision **Byeong Hyeok Choi:** Writing - Investigation, Conceptualization, Original Draft, Formal analysis, Visualization, Project administration **Wei Dai:** Writing - Writing - Conceptualization Original Draft, Funding acquisition, Project administration

Keywords

Aryl Hydrocarbon Receptor; Hydrogen peroxide; Cytochrome P450; Tryptophan; Oxindole; Oxidative Stress; IDO1; PD-L1

Introduction

The aryl hydrocarbon receptor (AhR) is an evolutionarily conserved ligand-dependent transcription factor [1]. AhR was initially characterized as a transcription factor regulating responses to xenobiotics [2]. In the absence of a ligand, AhR aggregates with other chaperone proteins in the cytoplasm and ligand binding triggers the translocation of AhR into the nucleus where it heterodimerizes with Aryl hydrocarbon Receptor Nuclear Translocator (ARNT) [3], forming an active transcription complex. The AhR/ARNT complex recognizes xenobiotic-responsive elements (XREs) and transactivates expression of a superfamily of metabolizing enzymes known as cytochrome P450 enzymes including CYP1A1, CYP1A2, and CYP1B1 [4].

Extensive research in the past two decades leads to the realization that AhR functions far beyond metabolism of xenobiotic compounds. In fact, AhR possesses essential physiological functions including development, metabolic homeostasis, and DNA damage responses [5–7]. As the transcription factor, AhR also controls expression of immune checkpoint proteins, thus functioning as an important component in mediating immune tolerance and immune suppression [8, 9]. For example, AhR is involved in transcriptional activation of PD-1 and PD-L1, two important immune checkpoint proteins [10, 11]. PD-L1 is highly expressed in a fraction of tumor cells [12]. PD-L1 expressed on tumor cells physically engages with PD-1 on T lymphocytes, leading to suppression of T cell cytotoxicity [13]. AhR also transactivates indoleamine 2’3’-dioxygenase 1 (IDO1), an enzyme also involved in immune suppression [14]. IDO1 functions to enzymatically converts tryptophan (Trp) into kynurenine (Kyn), the latter being an oncometabolite because of its ability to suppress T cell cytotoxicity in the tumor microenvironment by depletion of Trp [15].

Reactive oxygen species (ROS) are by-products of metabolism of oxygen, and they are essential in normal homeostasis [16]. However, an excess amount of ROS due to exposure to environmental toxicants or deregulated metabolic processes can be harmful or detrimental to organisms. It has been shown that ultraviolet light (UV) irradiation elicits ROS production in cells [17]. UV-induced generation of ROS is partly mediated through up-regulating the synthesis of nitric oxide synthase [18]. Moreover, it is known that UV (UVA and UVB) induces the photo-conversion of Trp into 6-Formylindolo[3,2-b]carbazole (FICZ), a potent AhR agonist [19]. It is also known that malignantly transformed cells contain an elevated level of ROS, which are thought to facilitate the survival and growth of tumor cells in the tumor microenvironment [20].

We are interested in the functional interaction between ROS and AhR, an environmental sensor molecule. We showed that treatment of HaCaT cells with H_2O_2 induced expression of CYP1A2 which depended on AhR. We also identified oxindole as a compound whose concentration in the culture medium was significantly increased after treatment with H_2O_2.

Oxindole was capable of inducing expression of CYP1A2 in a concentration- and AhR-dependent manner. Furthermore, we showed that H_2O_2 and oxindole induced expression of IDO1 and PD-L1 in multiple cell types, suggesting that oxidative stress may compromise immune responses in the tumor microenvironment through perturbing the AhR signaling axis.

Materials and methods

Cell culture and chemicals

HaCaT (immortalized human keratinocytes) and A549 (lung adenocarcinoma) cells were cultured in Dulbecco's Modified Eagle's Medium (DMEM, Corning, NY) supplemented with 10% fetal bovine serum (Atlanta biologicals) and 1% antibiotic/antimycotic (GIBCO™) and seeded 1×10^5 in a 100 mm cell culture dish (Corning, NY).

Hydrogen peroxide was purchased from Thermo Fisher Scientific (Waltham, MA) Hexavalent chromium, 2-oxindole, L-kynurenine, 6-formylindolo(3,2-b) carbazole-(FICZ), CH-223191 (an AhR antagonist) were all purchased from Sigma (St. Louis, MO).

Cell lysate preparation and immunoblotting

All cell samples were rinsed once with ice-cold PBS before harvesting. Cells were lysed in a RIPA buffer [50 mM Tris-HCl (pH 7.5), 150 mM NaCl, 1% IGEPAL, 0.1% SDS, and 0.5% sodium deoxycholate, 10 mM β-glycerophosphate, 1 mM DTT, 1 mM Na_3VO_4, 1 mM PMSF, 0.001x protease inhibitors, and Benzonase (Pierce™, 88700)], or cell lysis buffer [10 mM Tris-HCl (pH 7.4)] containing 1% SDS (Sigma-Aldrich) and 1 mM Na_3VO_4 (Fisher Scientific Co.). Cells mixed with the RIPA lysis buffer were incubated on ice for 30 min with gentle vortex every 10 min. Cell lysates were subjected to centrifugation at 4°C at 15,000 RCF for 10 min. After centrifugation, the supernatant was collected, and protein concentrations were determined with the use of Pierce™ BCA protein assay kit (Thermo Fisher Scientific, Inc.) according to the manufacturer's protocol.

Specific signals were visualized using enhanced chemiluminescence (ECL, Pierce), or Enhanced Chemifluorescence (ECF, Amersham) acquired by scanning with a phospho-imager (Typhoon FLA 7000, GE). Antibodies against CYP1A2 (D1tkt5), AHR (A-3) were purchased from Santa Cruz Biotechnology (Santa Cruz, CA). Antibodies against GAPDH (14C10), HIF-1β/ARNT(D28F3), IDO-1(D5J4E), PD-L1(E1L3N), Nrf2(D1Z9C), HO-1(E3F4S), NQO1(A180) and PARP-1 were purchased from Cell Signaling Technology (Danvers, MA). Antibody against tubulin was purchased from Proteintech (Rosemont, IL). Antibody against vinculin(MAB374) was purchased from Millipore. For western blot quantification, imageJ was used to measure blot integrated density.

Quantifications of Western Blots with ImageJ

All western blots quantifications with ImageJ reflect the relative amounts as a ratio of each protein band relative to the lane's loading control. All western blot data films are scanned with high resolution (300 dpi) and performed in ImageJ. All blot values are measured by integrated density then record in excel file (Supplement Dataset S1).

Real-Time PCR

HaCaT cells were lysed in a Trizol solution and total RNAs were isolated with ethanol precipitation. RNAs (400 ng) from each treatment were used for subsequent analyses with real-time polymerase chain reaction (real-time PCR) using a kit from Applied Biosystems (Foster City, CA). In brief, aliquots of a master mix containing RNAs, specific primers (refer to Supplement Table 1 for details), and other components were dispensed into a plate for real-time PCR reactions according to instructions provided by the supplier. Each reaction was carried out in triplicates. Specific conditions for PCR were as follows: 15 sec at 95°C and 1 min at 60°C, which were performed for 40 cycles. After that, samples were denatured by heating. Signals (mRNA expression) of each gene of interest relative to those of β-actin mRNA in each sample was determined using the $2^{-\Delta\Delta CT}$ method. Raw Ct values of qRT-PCR data are shown in Supplement Dataset S2. All RT-qPCR data are means ± SEM of three independent experiments performed in triplicate.

Gene silencing by siRNA

AhR siRNAs, Nrf2 siRNAs and control siRNAs were separately purchased from Dharmacon and Thermo fisher. HaCaT Cells seeded at 50% confluency in an antibiotic-free culture medium were transfected with siRNA duplexes specific for AhR, Nrf2 or control at a final concentration of 100 nM for 24 h using DharmaFECT I. The transfected cells were then incubated at 37°C in 5% CO_2 with 90% humidity. Transfected cells were collected and lysed for immunoblotting as described above.

Flow cytometry

Cells were seeded 1×10^6 in 60mm dishes with the complete medium until they reached about 60% confluence at the time of treatment. Cr(IV) treated cells were incubated with Cell-ROX (Invitrogen) dye for 30min. Cells were then collected and washed with 0.1% BSA / 1x PBS. All samples were filtered and analyzed on BD LSRII flow cytometer. Flow cytometric data were analyzed using FlowJo v10 software.

Mass spectrometry

Mass spectrometry was performed in conjunction with the Metabolomics Core Resource Lab facility of Grossman School of Medicine. Samples were analyzed on the hydrophobic/nonpolar platform with a custom skeleton input for the previously validated targeted compounds. The data were analyzed by manual annotation, principal components analysis, unsupervised hierarchical clustering, volcano plots, and other statistical comparisons. For untargeted analysis, the available MS/MS spectra were broadly searched against an upgraded data analysis pipeline which now includes both the NIST17MS/MS and METLIN spectral library database, as well as tolerating multiple ion types for a given metabolite. The resulting data were analyzed by principal components analysis, unsupervised hierarchical clustering, volcano plots, and other statistical comparisons. For targeted analysis, 2-oxindole, 6-formylindolo[3,2-b] carbazole (FICZ), tryptophan, and kynurenine were extracted in a 10 μM cocktail and run inside of the control block during LC/MS data acquisition to ensure that the compounds were not lost during the extraction phase. Each compound survived extraction, and each peak was isolated at the expected retention value. For all analysis,

instrument performance was assessed using the internal standards added to the samples during metabolite extraction. The raw values of mass spectrum are shown in Supplement Dataset S3.

Cell lysate fractionation

Cytosolic and nuclear extracts were obtained as described previously [21]. In brief, cell extracts were prepared in the harvest buffer (10 mm HEPES (pH 8.0), 50 mm NaCl, 0.5 m sucrose, 0.1 m EDTA, 0.5% Triton X-100) containing both protease inhibitors (1 mm dithiothreitol (DTT), 2 mg/ml pepstatin, 4 mg/ml aprotinin, 100 mm PMSF) and phosphatase inhibitors (10 mm tetrasodium pyrophosphate, 100 mm NaF, 17.5 mm β-glycerophosphate). The low speed supernatant (500 × g) containing cytoplasmic proteins was collected, and nuclear extracts were made by vortexing the nuclei for 15 min at 4 °C in a buffer containing 20 mm HEPES (pH 7.9), 400 mm NaCl, 1 mm EDTA, 1 mm EGTA, 0.1% IGEPAL CA-630, and protease inhibitors. Protein concentrations were measured using the bicinchoninic acid protein assay reagent kit (Pierce). Equal amounts of protein lysates from various samples were used for SDS-PAGE analysis followed by immunoblotting. Specific signals on immunoblots (polyvinylidene difluoride) were visualized using enhanced chemiluminescence (ECL, Pierce).

Statistical analysis

The Mann-Whitney test was conducted to evaluate the statistical significance of the difference in each treatment. The Kruskal–Wallis test (one-way non-parametric ANOVA) is used for comparing two or more independent samples of equal or different sample sizes. Statistical analyses were performed using SPSS version 24 (IBM Corporation, New York, NY) and GraphPad Prizm 9 (GraphPad Software, San Diego, CA). All data was graphed as mean ± SEM of independent experiments performed in triplicate. P value of less than 0.05 was considered statistically significant.

Results

Oxidative stress activates AhR

Given that oxidative stress exerted by UVB induces the generation of FICZ [22], a potent AhR ligand, we investigated the relationship between cellular oxidative stress and AhR activation. HaCaT cells were directly treated with H_2O_2 at various final concentrations for 24 h. Cell lysates were blotted for AhR and CYP1A2, the latter being a classical transcription target of AhR [23]. We observed that CYP1A2 expression was induced by H_2O_2 in a concentration-dependent manner, peaking around 0.5 mM (Fig. 1A). We then treated these cells with H_2O_2 (0.2 mM) for various times. We observed that H_2O_2 induced CYP1A2 expression in a time-dependent manner (Fig. 1B). Interestingly, H_2O_2 also increased AhR protein levels. To determine whether the increase in expression of AhR and its downstream target occurred at the transcription level, we measured mRNA levels in cells treated with the oxidant using real-time PCR. We observed that mRNA levels of CYP1A1, CYP1B1, and CYP1A2 were all briefly increased about 4 h after H_2O_2 treatment and then greatly elevated 24 h after the treatment. (Fig. 1C). Intriguingly, AhR mRNA level was slightly increased after H_2O_2 treatment for 4 h and stable in the later time points. To

determine whether CYP1A2 expression induced by H_2O_2 was AhR-dependent, we treated HaCaT cells with H_2O_2 in the presence or absence of CH233191, an AhR antagonist [24]. We observed that CH233191 completely suppressed CYP1A2 induction by H_2O_2, indicating that the induced expression of CYP1A2 depends on AhR (Fig. 1D).

Hexavalent chromium [Cr(VI)] is a well-known environmental carcinogen [25]. Upon entering cells, Cr(VI) undergoes rapid reduction to chromium (V) and chromium (III), which is accompanied by the generation of reactive oxygen species including superoxide [26]. Superoxide is known to be converted to H_2O_2 by the action of superoxide dismutase [27]. To confirm our assertion that hexavalent chromium induces oxidative stress, we detected cellular ROS generation with various hexavalent chromium concentrations by flow cytometry. Flow cytometry data indicated that hexavalent chromium elevated cellular ROS level at the sub-micromolar concentrations (Fig. 2A). Given the connection, we treated HaCaT cells with various concentrations of Cr(VI) for 24 h. We observed that expression of both AhR and CYP1A2 was increased after Cr(VI) treatment and that their levels of expression were correlated with Cr(VI) concentrations (Fig. 2B). Subsequent experiments demonstrated that AhR and CYP1A2 expression induced by Cr(VI) was time-dependent as well (Fig. 2C).

To determine whether induced expression of CYP1A2 depended on AhR, we transfected HaCaT cells with AhR siRNAs, or with control siRNAs, for 24 h before treatment with Cr(VI). We observed that downregulation of AhR by RNA interference compromised the induction of CYP1A2 by Cr(VI) (Fig. 2D), suggesting that AhR is essential in regulating increased expression of CYP1A2 after Cr(VI) treatment. To further determined whether induced expression of CYP1A2 by Cr(VI) depended on AhR, we treated HaCaT cells with Cr(VI) in the presence or absence of CH233191. We observed that the basal and Cr(VI)-induced levels of CYP1A2 were completely suppressed by CH233191 (Fig. 2E), again supporting the notion that Cr(VI)-induced expression of CYP1A2 is dependent on AhR signaling.

Preincubation of culture medium with H_2O_2 accelerates AhR activation

Nrf2 is known to function as a master transcription factor in response to the oxidative stress [28]. To differentiate the roles of AhR and Nrf2 in response to the oxidative stress, we transfected HaCaT cells with Nrf2 siRNAs, or with control siRNAs, for 24 h before treatment with H_2O_2. We showed that downregulation of Nrf2 by RNA interference compromised expression of Nrf2 downstream target genes including NQO1 and HO-1 (Fig. 3A), indicating that Nrf2 transactivation capacity was inhibited. However, increased expression of CYP1A2 induced by H_2O_2 was not significantly affected by Nrf2 silencing (Fig. 3A). These combined results thus strongly suggest that induction of CYP1A2 by H_2O_2 is largely mediated by the AhR signaling axis, but not the Nrf2 activation.

Given that neither H_2O_2 nor Cr(VI) are known AhR ligands, we speculated that these oxidants might provide a condition for the generation of an AhR agonist(s) in the culture medium. To test this possibility, we preincubated the medium with H_2O_2 for 30 min and then added the medium to the HaCaT cell culture. We observed that AhR expression was rapidly induced by H_2O_2* (namely, H_2O_2-preincubated medium for 30 min), peaking

around 8 h post-treatment (Fig. 3B). The AhR increase was immediately followed by the induction of CYP1A2. These results suggest that an AhR ligand(s) is generated during H_2O_2 pre-incubation, which in turn activates AhR and its signaling axis.

Upon ligand binding, AhR undergoes nuclear translocation where it interacts with ARNT, forming an active transcription complex [3]. To determine whether CYP1A2 induction was correlated with AhR nuclear translocation, we treated HaCaT cells with H_2O_2* for 1.5, 3, and 6 h, respectively. As a positive control, we also treated these cells with TCDD for 6 h. We fractionated cells into both cytoplasmic and nuclear parts. We observed that nuclear AhR peaked around 1.5 h after H_2O_2* treatment, which was followed by increased expression of CYP1A2 in the cytoplasm (Fig. 3C). Protein fractionation was efficient as revealed by blotting with compartment-specific markers tubulin (cytoplasmic) and PARP-1 (nuclear), respectively. To further determine whether H_2O_2*-induced expression of CYP1A2 depended on AhR, we employed both pharmacological and genetic approaches as described above. We observed that specific knockdown of AhR with siRNAs suppressed induction of CYP1A2 by H_2O_2* (Fig. 3D). Consistent with this, treatment with CH233191 also blocked the induction of CYP1A2 by H_2O_2* (Fig. 3D)

Oxindole as an AhR ligand generated by H_2O_2

Several Trp metabolic/catabolic products function as AhR ligands that include FICZ and kynurenine [22] [29]. Given the observation that the culture medium preincubated with H_2O_2 rapidly activates the AhR signaling pathway, we postulated that the strong oxidant might induce an AhR ligand(s) in the medium which was rich in Trp. Subsequent mass spectrometric analysis revealed no significant increase of FICZ in the H_2O_2-treated medium (data not shown). On the other hand, we noticed that oxindole was significantly increased in the H_2O_2-preincubated culture medium (Figure 4A and 4B). Given that oxindole is also a Trp metabolic product [30], we directly tested whether it was capable of activating AhR signaling. We treated HaCaT cells with 2-oxindole (a major form of oxindole) at various final concentrations for 24 h. We showed that 2-oxindole induced expression of CYP1A2 in a concentration- and time-dependent manner (Fig. 4C & 4D). Moreover, CYP1A2 expression induced by 2-oxindole depended on the activity of AhR as treatment with CH233191 abolished CYP1A2 induction by the compound (Fig. 4E). These combined studies thus support our hypothesis that the strong oxidant H_2O_2 catalyzes the formation of new compounds including oxindole to activate the AhR signaling axis.

H_2O_2 and 2-oxindole stimulate expression of immune checkpoint proteins

AhR plays an important role in both innate and adaptive immunity, partly through mediating expression of immune checkpoint proteins including IDO1, PD-1 and PD-L1 [10, 11, 14]. We then determined whether the medium preincubated with H_2O_2 was capable of inducing expression of IDO1. We showed that IDO1 was induced by H_2O_2* in a time-dependent manner (Fig. 5A and B) and that the induction of IDO1 by H_2O_2* was dependent on AhR as co-treatment with CH233191 significantly suppressed the induction (Fig. 5C). To further investigate whether the increase in expression of IDO1 occurred at the transcription level, we measured mRNA levels in cells treated with the oxidant using real-time PCR. We observed that mRNA levels of IDO1 was significantly induced after oxidant treatment

and strongly suppressed by AhR antagonist, again supporting the notion that H2O2-induced expression of IDO1 is dependent on AhR signaling (Fig. 5D). We next determined the ability of 2-oxindole in induction of IDO1 expression. We showed that 2-oxindole induced expression of IDO1 in a concentration- and time-dependent fashion in HaCaT cells (Fig. 5E and 5F).

Given the importance of PD-L1 in mediating immune evasion of many types of tumor cells, we determined whether 2-oxindole had any effect on expression of PD-L1. We chose A549 cells as it expresses a low level of PD-L1. We showed that 2-oxindole induced expression of PD-L1, as well as IDO1, in A549 cells in a concentration-dependent fashion (Fig. 6A).

Since PD-L1 expression is inducible by interferon-γ (IFN-γ) [31, 32], we also treated A549 cells with 2-oxindole and/or IFN-γ. We observed that although IFN-γ alone induced PD-L1 expression co-treatment with 2-oxindole significantly boosted induction of PD-L1 expression by the cytokine (Fig. 6B). As expected, 2-oxindole induced expression of CYP1A2 in A549 cells but its induction was suppressed by IFN-γ treatment (Fig. 6B). Combined, this series of studies strongly suggest that 2-oxindole potentially functions as an important ligand in modulating expression of immune checkpoint genes *in vivo* and that the oxidative stress may significantly compromise immune responses via deregulating AhR signaling.

Discussion

One school of thoughts is that AhR functions as a ROS inducer [23]. For example, the increase in ROS parameters is observed in liver when AhR downstream targets including cytochrome P450 (CYP) enzymes are activated to metabolize chemical compounds during the detoxification process [33]. One major rationale for AhR as an oncogene is that ROS accumulation due to increased CYP activities, leading to severe oxidative stress and increased DNA damage, favoring malignant transformation [33, 34]. Several lines of recent evidence suggest that ROS play an essential role in activating AhR, thus enhancing expression of its downstream targets. In breast cancer cells, ROS accumulation strongly correlates with high AhR expression, triggering AhR nuclear translocation, and promoting its transcriptional activity [20]. In addition, UVB irradiation or hydrogen peroxide treatment causes the accumulation of FICZ, which is mediated by inhibitory effect of CYP enzymes, thereby activating AhR [35]. In the current study, we have obtained lines of new evidence that support ROS as AhR activators. We have found that the oxidative stress promotes the generation of oxindole, a newly-identified AhR agonist. Oxindole is also a Trp catabolic derivative and H_2O_2 can facilitate its generation from Trp *in vitro* [36]. It is generally thought that *in vivo* oxindole is derived from Trp through the activities of microbiome in the intestine [30].

Nrf2 is the major transcription factor regulating redox homeostasis [37]. Activated Nrf2 is translocated to the nucleus where it binds to antioxidant response elements (AREs), promoting transcription of genes involved in antioxidant activities including heme-oxygenase 1 (HO-1) and NAD(P)H: quinone oxidoreductase 1(NQO1) [38]. In our current study, we also analyzed Nrf2-mediated transactivation in Nrf2-silenced HaCaT cells treated

with H_2O_2. We observed that expression of HO-1 and NQO1 genes was induced by H_2O_2 treatment and that Nrf2 downregulation via RNA interference greatly suppressed expression of these genes, consistent with early observations that HO-1 and NQO1 genes are primarily regulated by Nrf2. Moreover, our current study reveals that ROS-induced expression of CYP1A2 was not significantly affected by Nrf2 downregulation (Fig. 3A), suggesting AhR, but not Nrf2, plays a major role in mediating CYP1A2 expression under the oxidative stress. On the other hand, Nrf2 is known to directly regulate expression of AhR [39]. Therefore, we speculate that ROS may modulate the AhR signaling pathway in two different manners: namely, (I) facilitating the generation of AhR ligands, and (II) transactivating AhR by Nrf2, leading to enhanced expression of AhR.

In our mass spectrometry analysis, we did not detect FICZ in the medium treated with H_2O_2, which may be partly due to a short treatment time. On the other hand, we have identified oxindole as a new compound in the culture medium whose concentration is quickly increased after H_2O_2 treatment. It is well known thar many environmental toxicants and carcinogens are capable of inducing ROS including superoxide *in vivo* [40]. As superoxide is converted to hydrogen peroxide by superoxide dismutase [27], it is conceivable that H_2O_2 produced *in vivo* can lead to increased levels of oxindole, thus activating the AhR signaling axis. Oxindole is a Trp-metabolic product, primarily derived from metabolism by intestinal microbiota [30]. It has been reported that oxindole can be predictive of the AhR activity in modulating gastrointestinal homeostasis and intestinal microbiome [30]. Thus, it is of significance that oxindole also functions as an AhR agonist given that AhR downstream targets include immune checkpoint components. Supporting this notion, we have shown that 2-oxindole induces expression of both IDO-1 and PD-L1. Therefore, it would be crucial to identify the presence and induction of oxindole (or its derivatives) *in vivo* under oxidative stress and study its role in the tumor microenvironment in various mouse models.

In conclusion, we have established a molecular connection between oxidative stress and AhR activation. Our observations suggest the following model that may explain the activation of AhR and its downstream signaling *in vivo* under oxidative stress (Fig. 7). Environmental factors including UV and various toxicants will elicit the production of ROS in cells whereas cellular metabolism also leads to the production of ROS *in vivo*. Hydrogen peroxide derived from ROS converts Trp into oxindole which in turn functions as an AhR agonist, activating its downstream signaling. Ligand-bound AhR associates with ARNT, forming an active transcriptional factor. The AhR/ARNT complex binds to specific *cis*-acting elements in the genome, transactivating expression of CYP family genes, as well as immune checkpoint genes including IDO1, PD-1, and PD-L1. High levels of expression of immune checkpoint genes in malignantly transformed cells lead to the suppression of T cell cytotoxicity.

Supplementary Material

Refer to Web version on PubMed Central for supplementary material.

Acknowledgments

We acknowledge NYU Langone Health's Metabolomics Laboratory for its help in acquiring and analyzing the data presented. The mass spectrometric experiments were supported in part by NIH grant U2C-DK119886. This work was supported in part by National Institutes of Health (NIH) grants R01CA213159 and R01CA216987 to W.D. and R01ES031402 to S.C.

Data availability statement

The proteomics data is deposited in the Metabolomics Workbench and can be accessed directly through this link: "directly via its Project DOI: http://dx.doi.org/10.21228/M8Z993.

References

1. Brinkmann V, et al. , The Aryl Hydrocarbon Receptor (AhR) in the Aging Process: Another Puzzling Role for This Highly Conserved Transcription Factor. Front Physiol, 2019. 10: p. 1561. [PubMed: 32009975]
2. Kou Z and Dai W, Aryl hydrocarbon receptor: Its roles in physiology. Biochem Pharmacol, 2021. 185: p. 114428. [PubMed: 33515530]
3. Swanson HI, DNA binding and protein interactions of the AHR/ARNT heterodimer that facilitate gene activation. Chem Biol Interact, 2002. 141(1–2): p. 63–76. [PubMed: 12213385]
4. Fujii-Kuriyama Y and Mimura J, Molecular mechanisms of AhR functions in the regulation of cytochrome P450 genes. Biochem Biophys Res Commun, 2005. 338(1): p. 311–7. [PubMed: 16153594]
5. Fujii-Kuriyama Y and Kawajiri K, Molecular mechanisms of the physiological functions of the aryl hydrocarbon (dioxin) receptor, a multifunctional regulator that senses and responds to environmental stimuli. Proc Jpn Acad Ser B Phys Biol Sci, 2010. 86(1): p. 40–53.
6. Tian J, et al. , The Aryl Hydrocarbon Receptor: A Key Bridging Molecule of External and Internal Chemical Signals. Environ Sci Technol, 2015. 49(16): p. 9518–31. [PubMed: 26079192]
7. Gim J, et al. , A system-level investigation into the cellular toxic response mechanism mediated by AhR signal transduction pathway. Bioinformatics, 2010. 26(17): p. 2169–75. [PubMed: 20610613]
8. Stockinger B, et al. , The aryl hydrocarbon receptor: multitasking in the immune system. Annu Rev Immunol, 2014. 32: p. 403–32. [PubMed: 24655296]
9. Xue P, Fu J, and Zhou Y, The Aryl Hydrocarbon Receptor and Tumor Immunity. Front Immunol, 2018. 9: p. 286. [PubMed: 29487603]
10. Kenison JE, et al. , The aryl hydrocarbon receptor suppresses immunity to oral squamous cell carcinoma through immune checkpoint regulation. Proc Natl Acad Sci U S A, 2021. 118(19).
11. Wang GZ, et al. , The Aryl hydrocarbon receptor mediates tobacco-induced PD-L1 expression and is associated with response to immunotherapy. Nat Commun, 2019. 10(1): p. 1125. [PubMed: 30850589]
12. Sampedro-Nunez M, et al. , Analysis of expression of the PD-1/PD-L1 immune checkpoint system and its prognostic impact in gastroenteropancreatic neuroendocrine tumors. Sci Rep, 2018. 8(1): p. 17812. [PubMed: 30546030]
13. Peng Q, et al. , PD-L1 on dendritic cells attenuates T cell activation and regulates response to immune checkpoint blockade. Nat Commun, 2020. 11(1): p. 4835. [PubMed: 32973173]
14. Wirthgen E and Hoeflich A, Endotoxin-Induced Tryptophan Degradation along the Kynurenine Pathway: The Role of Indolamine 2,3-Dioxygenase and Aryl Hydrocarbon Receptor-Mediated Immunosuppressive Effects in Endotoxin Tolerance and Cancer and Its Implications for Immunoparalysis. J Amino Acids, 2015. 2015: p. 973548. [PubMed: 26881062]
15. Mbongue JC, et al. , The Role of Indoleamine 2, 3-Dioxygenase in Immune Suppression and Autoimmunity. Vaccines (Basel), 2015. 3(3): p. 703–29. [PubMed: 26378585]
16. Zorov DB, Juhaszova M, and Sollott SJ, Mitochondrial reactive oxygen species (ROS) and ROS-induced ROS release. Physiol Rev, 2014. 94(3): p. 909–50. [PubMed: 24987008]

17. Panich U, et al. , Ultraviolet Radiation-Induced Skin Aging: The Role of DNA Damage and Oxidative Stress in Epidermal Stem Cell Damage Mediated Skin Aging. Stem Cells Int, 2016. 2016: p. 7370642. [PubMed: 27148370]
18. de Jager TL, Cockrell AE, and Du Plessis SS, Ultraviolet Light Induced Generation of Reactive Oxygen Species. Adv Exp Med Biol, 2017. 996: p. 15–23. [PubMed: 29124687]
19. Syed DN and Mukhtar H, FICZ: A Messenger of Light in Human Skin. J Invest Dermatol, 2015. 135(6): p. 1478–1481. [PubMed: 25964268]
20. Kubli SP, et al. , AhR controls redox homeostasis and shapes the tumor microenvironment in BRCA1-associated breast cancer. Proc Natl Acad Sci U S A, 2019. 116(9): p. 3604–3613. [PubMed: 30733286]
21. Choi BH, et al. , Cdh1, a Substrate-recruiting Component of Anaphase-promoting Complex/Cyclosome (APC/C) Ubiquitin E3 Ligase, Specifically Interacts with Phosphatase and Tensin Homolog (PTEN) and Promotes Its Removal from Chromatin*. Journal of Biological Chemistry, 2014. 289(25): p. 17951–17959. [PubMed: 24811168]
22. Smirnova A, et al. , Evidence for New Light-Independent Pathways for Generation of the Endogenous Aryl Hydrocarbon Receptor Agonist FICZ. Chem Res Toxicol, 2016. 29(1): p. 75–86. [PubMed: 26686552]
23. Vogel CFA, et al. , The aryl hydrocarbon receptor as a target of environmental stressors - Implications for pollution mediated stress and inflammatory responses. Redox Biol, 2020. 34: p. 101530. [PubMed: 32354640]
24. Zhao B, et al. , CH223191 is a ligand-selective antagonist of the Ah (Dioxin) receptor. Toxicol Sci, 2010. 117(2): p. 393–403. [PubMed: 20634293]
25. Holmes AL, Wise SS, and Wise JP Sr., Carcinogenicity of hexavalent chromium. Indian J Med Res, 2008. 128(4): p. 353–72. [PubMed: 19106434]
26. Wise JP Jr., et al. , Current understanding of hexavalent chromium [Cr(VI)] neurotoxicity and new perspectives. Environ Int, 2022. 158: p. 106877. [PubMed: 34547640]
27. Wang Y, et al. , Superoxide dismutases: Dual roles in controlling ROS damage and regulating ROS signaling. J Cell Biol, 2018. 217(6): p. 1915–1928. [PubMed: 29669742]
28. Ma Q, Role of nrf2 in oxidative stress and toxicity. Annu Rev Pharmacol Toxicol, 2013. 53: p. 401–26. [PubMed: 23294312]
29. Kaiser H, Parker E, and Hamrick MW, Kynurenine signaling through the aryl hydrocarbon receptor: Implications for aging and healthspan. Exp Gerontol, 2020. 130: p. 110797. [PubMed: 31786316]
30. Dong F, et al. , Intestinal microbiota-derived tryptophan metabolites are predictive of Ah receptor activity. Gut Microbes, 2020. 12(1): p. 1–24.
31. Garcia-Diaz A, et al. , Interferon Receptor Signaling Pathways Regulating PD-L1 and PD-L2 Expression. Cell Rep, 2019. 29(11): p. 3766. [PubMed: 31825850]
32. Garcia-Diaz A, et al. , Interferon Receptor Signaling Pathways Regulating PD-L1 and PD-L2 Expression. Cell Rep, 2017. 19(6): p. 1189–1201. [PubMed: 28494868]
33. Dostalek M, et al. , Development of oxidative stress by cytochrome P450 induction in rodents is selective for barbiturates and related to loss of pyridine nucleotide-dependent protective systems. J Biol Chem, 2008. 283(25): p. 17147–57. [PubMed: 18442974]
34. Zhou D, Shao L, and Spitz DR, Reactive oxygen species in normal and tumor stem cells. Adv Cancer Res, 2014. 122: p. 1–67. [PubMed: 24974178]
35. Wincent E, et al. , Inhibition of cytochrome P4501-dependent clearance of the endogenous agonist FICZ as a mechanism for activation of the aryl hydrocarbon receptor. Proc Natl Acad Sci U S A, 2012. 109(12): p. 4479–84. [PubMed: 22392998]
36. Itakura K, Uchida K, and Kawakishi S, Selective formation of oxindole- and formylkynurenine-type products from tryptophan and its peptides treated with a superoxide-generating system in the presence of iron(III)-EDTA: a possible involvement with iron-oxygen complex. Chem Res Toxicol, 1994. 7(2): p. 185–90. [PubMed: 8199307]
37. Nguyen T, Nioi P, and Pickett CB, The Nrf2-antioxidant response element signaling pathway and its activation by oxidative stress. J Biol Chem, 2009. 284(20): p. 13291–5. [PubMed: 19182219]

38. da Costa RM, et al. , Nrf2 as a Potential Mediator of Cardiovascular Risk in Metabolic Diseases. Frontiers in Pharmacology, 2019. 10.

39. Shin S, et al. , NRF2 modulates aryl hydrocarbon receptor signaling: influence on adipogenesis. Mol Cell Biol, 2007. 27(20): p. 7188–97. [PubMed: 17709388]

40. Liou GY and Storz P, Reactive oxygen species in cancer. Free Radic Res, 2010. 44(5): p. 479–96. [PubMed: 20370557]

Highlights

- ROS increases the AhR activity, and enhances the expression of CYP genes.
- 2-oxindole is identified as a tryptophan catabolic product by ROS.
- ROS enhances expression of CYP1A2 in an AhR-dependent manner.
- ROS and 2-oxindole induces expression of IDO1 and PD-L1.
- ROS play a crucial role in immune suppression via perturbing AhR signaling.

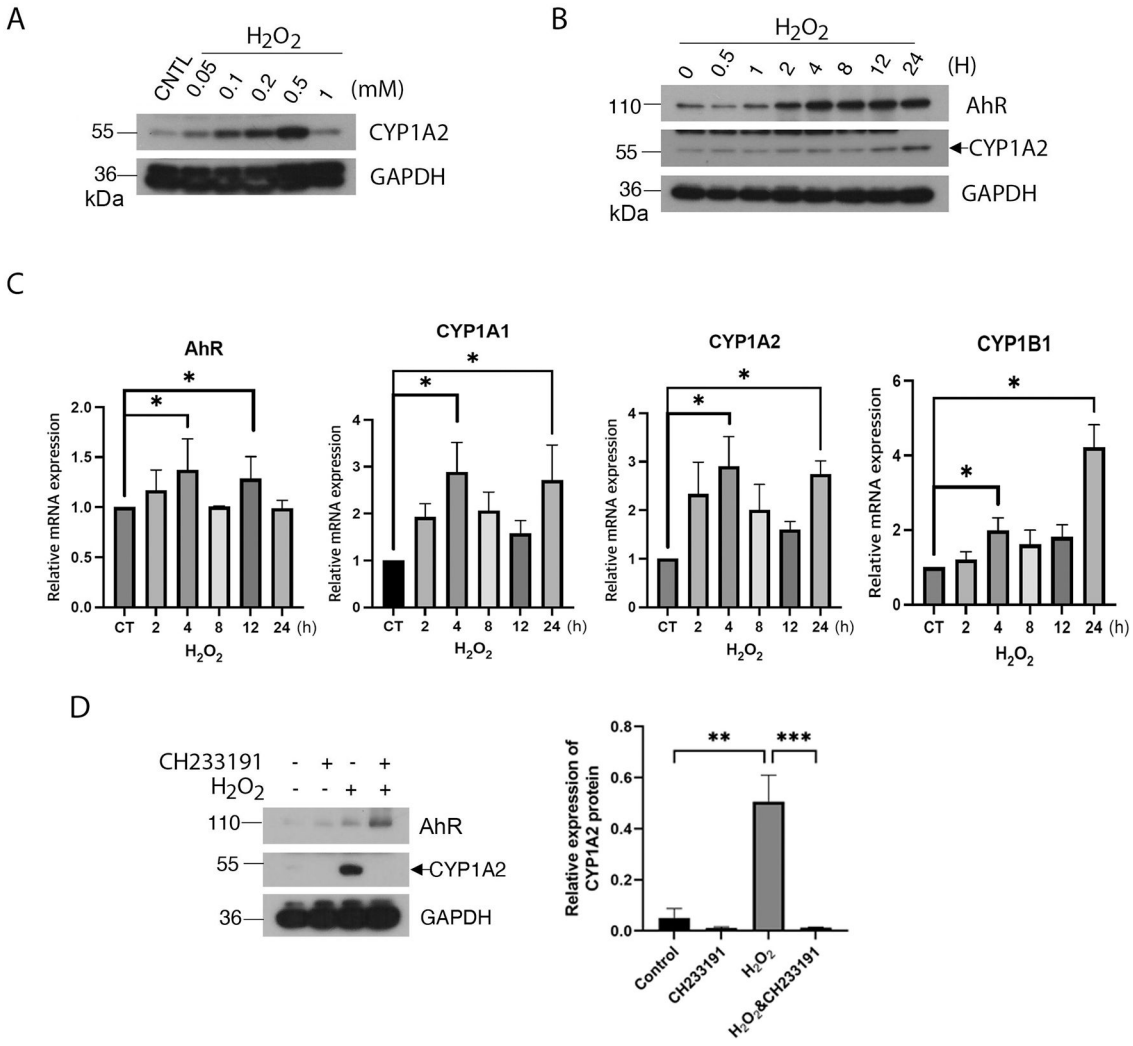

Figure 1.

Oxidative stress activates AhR. (A) HaCaT cells were treated with various concentrations of H_2O_2 for 24 h. Equal amounts of cell lysates were blotted for CYP1A2 and GAPDH. (B) HaCaT cells were treated with H_2O_2 (0.2 mM) for various times as indicated. Equal amounts of cell lysates were blotted for AhR, CYP1A2 and GAPDH. (C) HaCaT cells were treated with H_2O_2 (0.2 mM) for various times as indicated. Total RNAs were isolated. Levels of mRNAs for AhR, CYP1A1, CYP1B1, and CYP1A2 were analyzed by real-time PCR analysis as described Materials and Methods. (D) HaCaT cells were treated with H_2O_2 for 24 h in the presence or absence of CH233191, an AhR antagonist. Equal amounts of cell lysates were blotted for AhR, CYP1A2, and GAPDH. Western blot (left) is representative of one experiment and triplicated western blot quantifications (right) were analyzed by statistical analysis as described Methods.

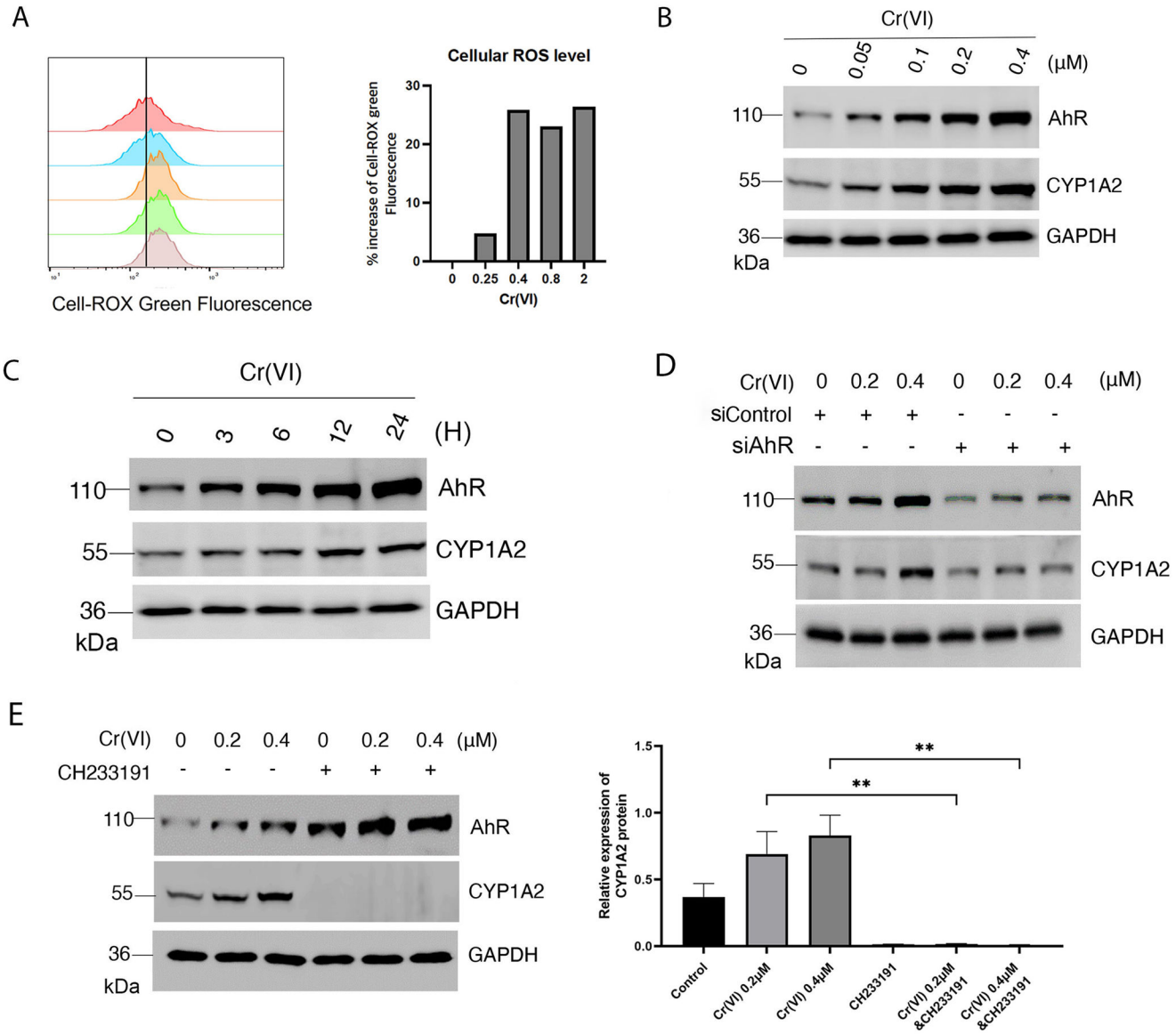

Figure 2.

Hexavalent chromium activates AhR. (A) HaCaT cells were treated with various concentrations of Cr(VI) as indicated. Levels of cellular ROS were measured and analyzed by flow cytometry as described Material and Methods. (B) HaCaT cells were treated with various concentrations of Cr(VI) as indicated. Equal amounts of cell lysates were blotted for AhR, CYP1A2 and GAPDH. (C) HaCaT cells were treated with Cr(VI) at 0.4 μM for various times as indicated. Equal amounts of cell lysates were blotted for AhR, CYP1A2 and GAPDH. (D) HaCaT cells were transfected with AhR-specific siRNAs or control siRNAs for 36 h before treatment with Cr(VI) for 24 h. At the end of experiments, cells were lysed and equal amounts of cell lysates were blotted for AhR, CYP1A2, and GAPDH. (E) HaCaT cells were treated with Cr(VI) (0.2 μM and 0.4 μM) in the presence or absence of CH233191 for 24 h. Equal amounts of cell lysates were blotted for AhR, CYP1A2, and

GAPDH. Western blot (left) is representative of one experiment and triplicated western blot quantifications (right) were analyzed by statistical analysis as described Methods.

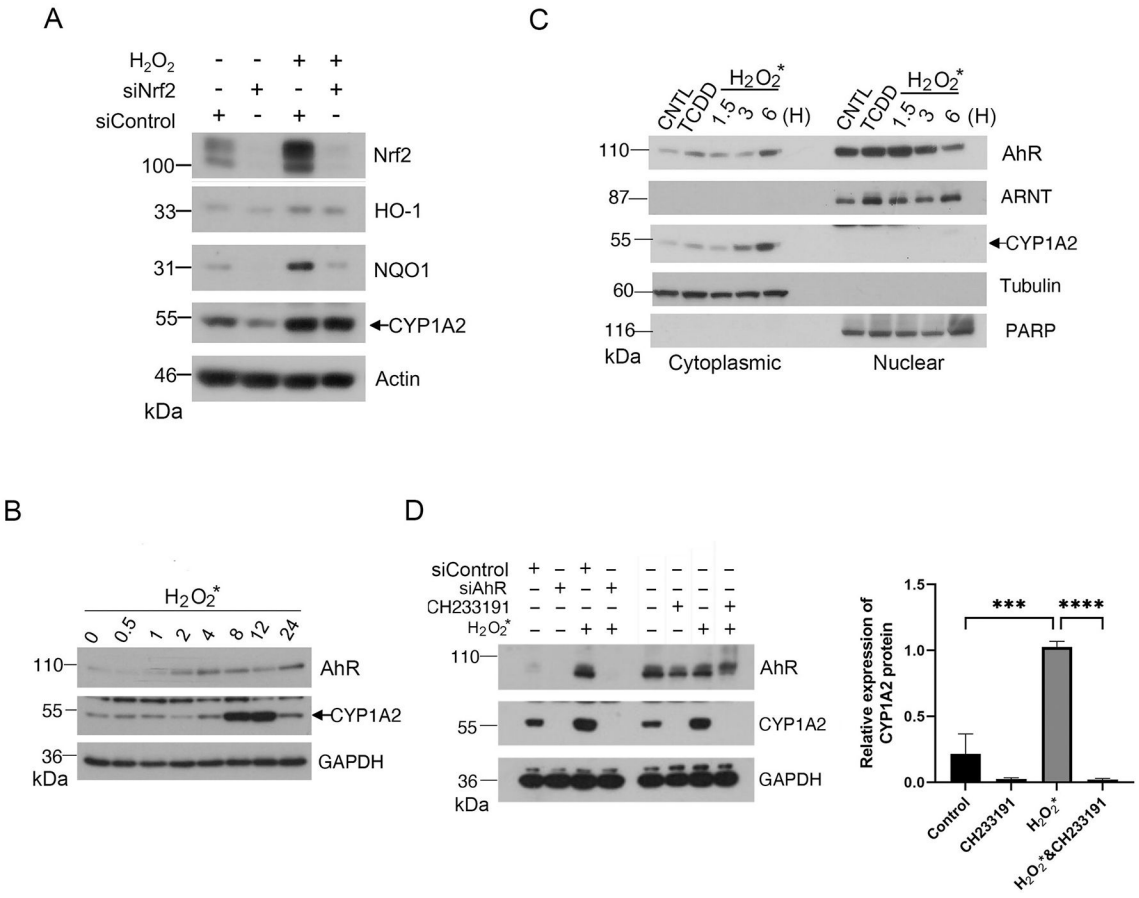

Figure 3.

Oxidant H_2O_2 induces an AhR agonist(s) in the culture medium. (A) HaCaT cells were transfected with Nrf2-specific siRNAs or control siRNAs for 24 h before treatment with H_2O_2 for 24 h. At the end of experiments, cells were lysed, and equal amounts of cell lysates were blotted for Nrf2, HO-1, NQO1, CYP1A2, and actin. (B) H_2O_2 (at a final concentration of 0. 2 mM) was supplemented to the warmed culture medium (DMEM with FBS) for 30 min in dark before it (H_2O_2-containing medium) was added to HaCaT cells. Cells were incubated with H_2O_2-containing medium for various times before they were harvested for lysis. Equal amounts of cell lysates were blotted for AhR, CYP1A2 and GAPDH. (C) HaCaT cells were treated with H_2O_2 for 1.5, 3, or 6 h before they were collected for fractionation into the cytoplasmic or nuclear parts. Cells treated with TCDD (5nM) or vehicle were also fractionated as control. Equal amounts of cell lysates of various treatments were blotted for AhR, ARNT, CYP1A2. Cell lysates were also blotted for compartmental markers including α-tubulin (cytoplasmic) and PARP-1 (nuclear). (D) HaCaT cells were transfected with AhR siRNAs or control siRNAs for 48 h before they were cultured in H_2O_2-pretreated medium for 8 h. HaCaT cells incubated in H_2O_2-pretreated medium were also treated with CH233191 or vehicle for 8 h. At the end of cultures, cells were collected and lysed. Equal amounts of cell lysates were blotted for AhR, CYP1A2 and GAPDH. Western blot (left) is representative of one experiment and triplicated western blot quantifications (right) were analyzed by statistical analysis as described Methods.

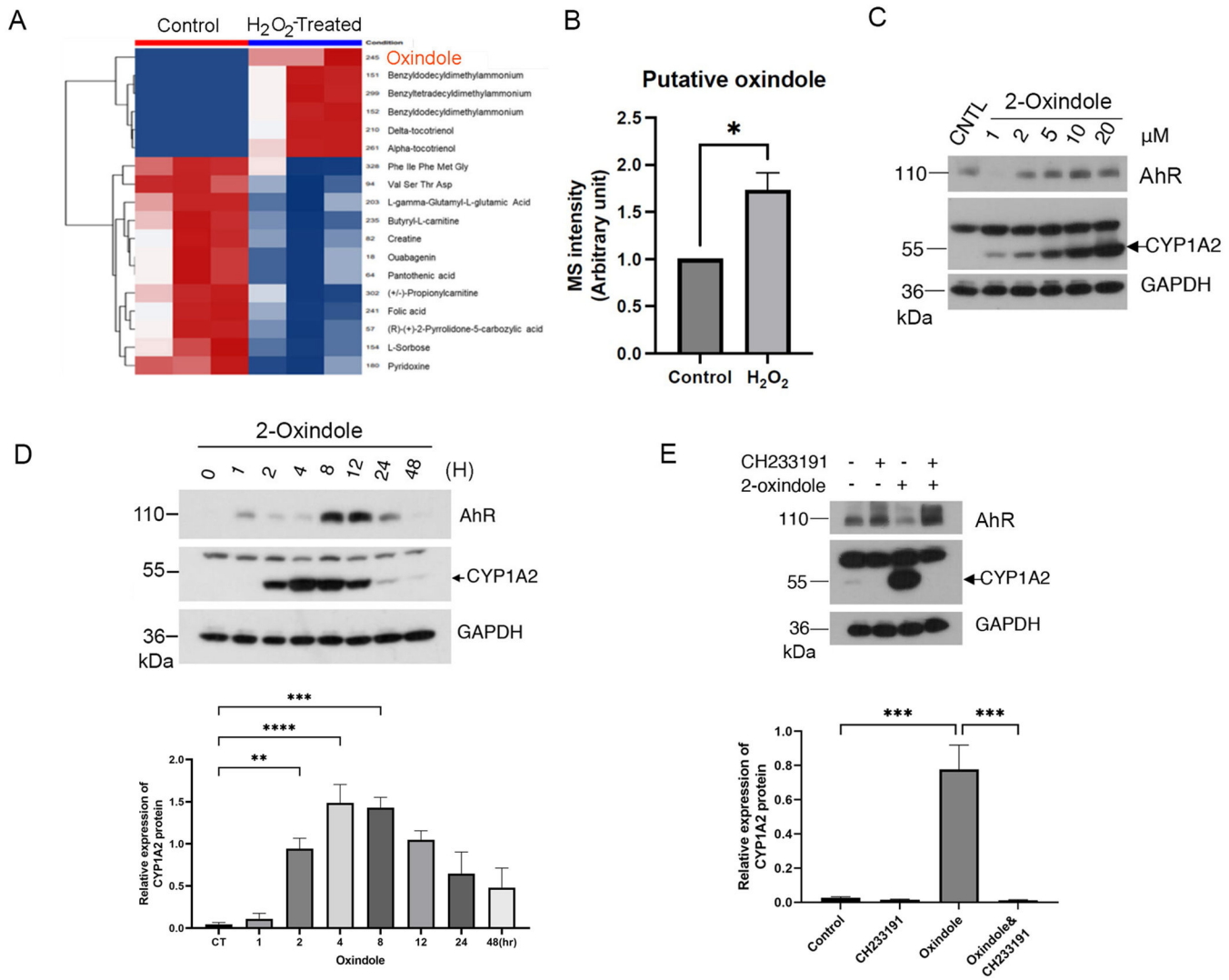

Figure 4.

Oxindole induced by H_2O_2 activates AhR. (A) Unsupervised clustering analysis of global metabolites in DMEM Medium (triplicates) vs. H_2O_2-treated DMEM medium (triplicates). Red color denotes those compounds increased in the samples whereas Blue color denotes the compounds that were decreased in H_2O_2-treated panels. (B) Mass spectrometric quantification of oxindole in control samples (medium with FBS) and treated samples (medium with FBS incubated with H_2O_2 for 30 min). (C) HaCaT cells were treated with 2-oxindole at various final concentrations, or treated with vehicle, for 24 h. Equal amounts of cell lysates were blotted for AhR, CYP1A2, and GAPDH. (D). HaCaT cells were treated with 2-oxindole (10 μM) or vehicle for various times as indicated. Equal amounts of cell lysates were blotted for AhR, CYP1A2, and GAPDH. (E) HaCaT cells were treated with 2-oxindole (10 μM) for 8 h in the presence or absence of CH233191. Equal amounts of cell lysates were blotted for AhR, CYP1A2, and GAPDH. Western blot (upper) is representative of one experiment and triplicated western blot quantifications (lower) were analyzed by statistical analysis as described Methods (D and E).

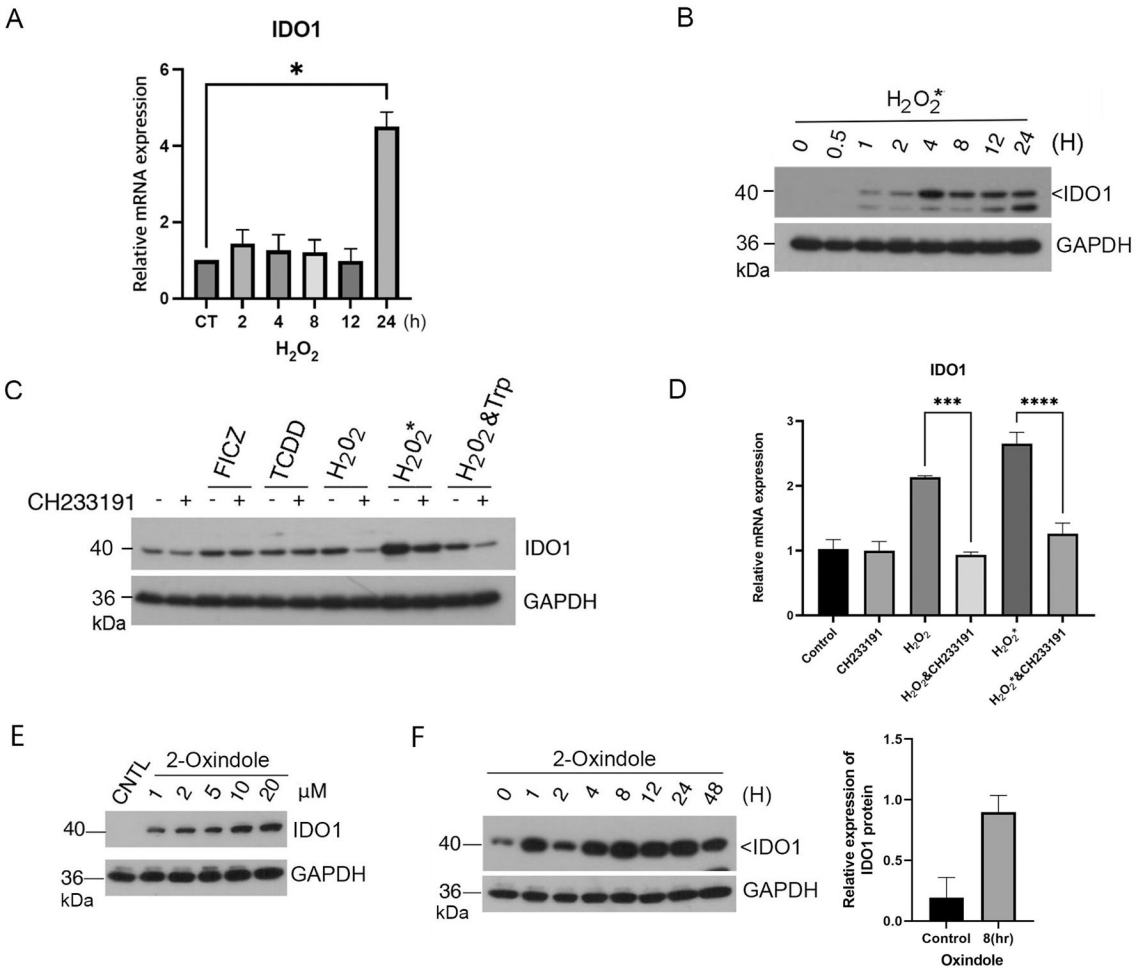

Figure 5.

H_2O_2 and 2-oxindole induce expression of immune checkpoint proteins. (A) HaCaT cells were treated with H2O2 (0.2 mM) for various times as indicated. Total RNAs were isolated. Levels of mRNAs for IDO1 was analyzed by real-time PCR analysis as described Materials and Methods. (B) HaCaT cells were treated with H_2O_2 (0.2 mM) for various times as indicated. Equal amounts of cell lysates were blotted for IDO1 and GAPDH. (C) HaCaT cells were treated with FICZ, TCDD, H_2O_2, H_2O_2* (medium preincubated with H_2O_2), or vehicle for 24 h in the presence or absence of CH233191. H_2O_2 either directly added to the cell culture or preincubated with the culture medium before adding to cells was used at the same final concentration of 0.2 mM. Equal amounts of cell lysates were blotted for IDO1 and GAPDH. Western blot is representative of one experiment and triplicated western blot quantifications were analyzed by statistical analysis as described Methods (D). (E) HaCaT cells were treated with 2-oxindole for 8 h at various concentrations as indicated. Equal amounts of cell lysates were blotted for IDO1 and GAPDH. (F) HaCaT cells were treated with 2-oxindole (10 μM) or vehicle for various times as indicated. Equal amounts of cell lysates were blotted for IDO1 and GAPDH. Western blot (left) is representative of one experiment and triplicated western blot quantifications (right) were analyzed by statistical analysis as described Methods.

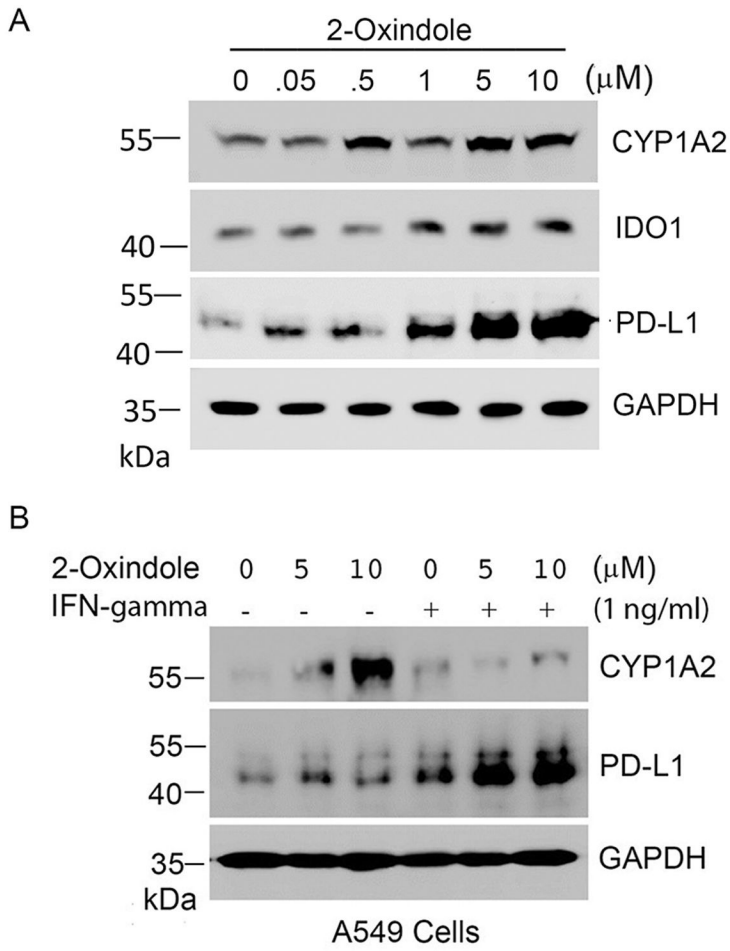

Figure 6.

Oxindole induces expression of PD-L1. (A) A549 cells were treated with 2-oxindole of various concentrations as indicated for 24 h after which cells were lysed. Equal amounts of cell lysates were blotted for CYP1A2, IDO1, PD-L1, and GAPDH. (B) A549 cells were treated with 2-oxindole (5 and 10 μM) and/or IFN-γ (1 ng/ml) as indicated for 24 h. Equal amounts of cell lysates were blotted for CYP1A2, PD-L1, and GAPDH.

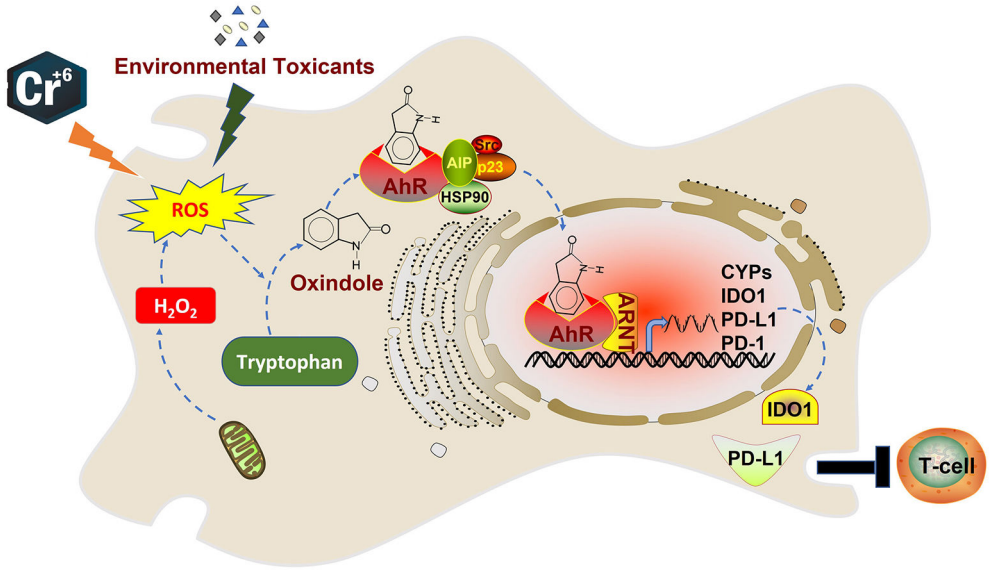

Figure 7.
A model depicting regulation of AhR and its signaling axis under oxidative stress.

Table 1.

Primers used for real-time PCR analyses.

Gene	Type	Description	Sequence
β-Actin	DNA	Forward	CTGGAACGGTGAAGGTGACA
	DNA	Reverse	AAGGGACTTCCTGTAACAATGCA
AhR	DNA	Forward	CAAATCCTTCCAAGCGGCATA
	DNA	Reverse	CGCTGAGCCTAAGAACTGAAAG
CYP1A1	DNA	Forward	AAGGGGCGTTGTGTCTTTGT
	DNA	Reverse	ATACACTTCCGCTTGCCCAT
CYP1B1	DNA	Forward	CTTCACCAGGTATCCTGATG
	DNA	Reverse	GCAGGCTCATTTGGGTTGGC
CYP1A2	DNA	Forward	CTTCGCTACCTGCCTAACCC
	DNA	Reverse	GACTGTGTCAAATCCTGCTCC
IDO1	DNA	Forward	TCTCATTTCGTGATGGAGACTGC
	DNA	Reverse	GTGTCCCGTTCTTGCATTTGC
GAPDH	DNA	Forward	GTCTCCTCTGACTTCAACAGCG
	DNA	Reverse	ACCACCCTGTTGCTGTAGCCAA